Proposed abstract for presentation at ICCFD4, Ghent, Belgium, July 10-14, 2006

Unsteady Flow Simulation of High-Speed Turbopumps

Cetin C. Kiris, Dochan Kwak, William Chan, and Jeffrey A. Housman
NASA Advanced Supercomputing Division (NAS)
NASA Ames Research Center, Moffett Field, CA 94035

Key Words: unsteady hydrodynamics, turbopump, high-end computing

1. Introduction

Computation of high-speed hydrodynamics requires high-fidelity simulation to resolve flow features involving transient flow, cavitation, tip vortex and multiple scales of unsteady fluctuations. One example of this type in aerospace is related to liquid-fueled rocket turbopump. Rocket turbopumps operate under severe conditions at very high rotational speeds typically at thousands of rpm. For example, the Shuttle orbiter low-pressure-fuel-turbopump creates transient flow features associated with reverse flows, tip clearance effects, secondary flows, vortex shedding, junction flows, and cavitation effects. Flow unsteadiness originating from the orbiter Low-Pressure-Fuel-Turbopump (LPFTP) inducer is one of the major contributors to the high frequency cyclic loading that results in high cycle fatigue damage to the flow liners just upstream of the LPFTP. The reverse flow generated at the tip of the inducer blades travels upstream and interacts with the bellows cavity. Simulation procedure for this-type high-speed hydrodynamic problems requires a method for quantifying multi-scale and multi-phase flow as well as an efficient high-end computing strategy. The current paper presents a high-fidelity computational procedure for unsteady hydrodynamic problems using a high-speed liquid-fueled rocket turbopump.

2. Computational Procedure

The incompressible Navier-Stokes flow solver based on the artificial compressibility method was used to compute the flow of liquid hydrogen in several test geometries including feed line and an inducer for pumping. All computations included tip leakage effects with a radial tip clearance of 0.006 inches, a pump operating condition of a mass flow rate of 154.7 lbm/sec, and a rotational speed of 15,761 rpm. One of the computational models is illustrated in Figure 1 which shows the LPFTP inducer with 4 long and 4 short blades, and a straight duct, which extends 4 duct diameters upstream of the inducer. The bull nose of the inducer, and split blades are included in the model. The objective of studying this model is to compare unsteady pressure values against experimental data. To resolve the complex geometry in relative motion, an overset grid approach is employed. The geometrically complex body is decomposed into a number of simple grid components. Connectivity between neighboring grids is established by interpolation at each grid outer boundaries. Addition of new components to the system and simulation of arbitrary relative motion between multiple bodies are achieved by establishing new connectivity without disturbing the existing grids. This computational grid has 57 overset zones with 26.1 Million grid points.

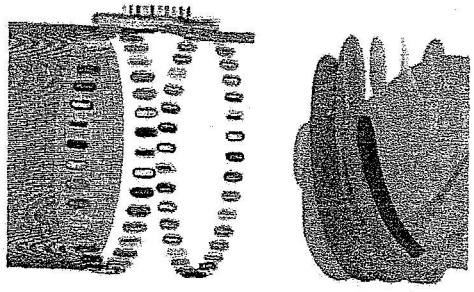

Figure 1. Surface grids for LPFTP and the LH2 feed line including circumferential holes upstream of the pump.

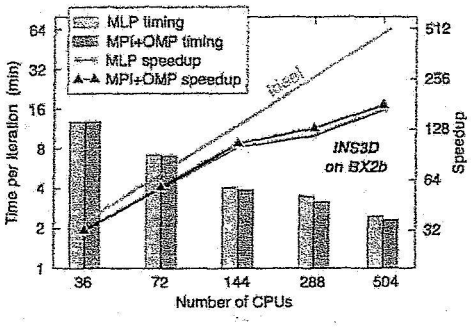

Figure 2. INS3D-MLP and MPI+OMP performance on Columbia platform.

The present computations are performed utilizing the INS3D computer code[1-3], which solves the incompressible Navier-Stokes equations for both steady-state and unsteady flows. To obtain time-accurate solutions, the equations are iterated to convergence in pseudo-time for each physical time step until the divergence of the velocity field has been reduced below a specified tolerance value. The total number of sub-iterations required varies depending on the problem, time step size and the artificial compressibility parameter used. Typically the number ranges from 10 to 30 sub-iterations.

The computational requirement for the model problem is big, and thus two distinct parallel processing paradigms have been implemented. These include the Multi-Level Parallel (MLP) and the MPI/OpenMP hybrid parallel programming models. Both models contain coarse and fine grain parallelism. Coarse grain parallelism is achieved through a UNIX fork in MLP and through explicit message passing in the MPI/OpenMP hybrid code. Fine grain parallelism is achieved using OpenMP compiler directives in both the MLP and MPI/OpenMP hybrid codes. Computations were performed to compare the scalability between the MLP and MPI/OpenMP hybrid versions of the INS3D code on the Columbia system using the BX2b processors. Figure 2 displays the time per iteration (in minutes) versus the number of CPUs for both the MLP and MPI/OpenMP hybrid versions of the code.

3. Computed Example

The Reynolds number for the calculations is 36 Million. The computed results show a significant time-periodic back-flow generated by the inducer reaching 15-20% of the tip velocity and a jet flow of 10-15% of the inducer tip speed which penetrates into the bellows cavity creating an unsteady recirculation region in the cavity. The reverse flow and unsteady recirculation regions create an unsteady interaction between the duct of the feed line and the cavity region just upstream of the inducer resulting in high frequency cycle loading on the feed line structure. The back-flow also creates swirl in the cavity on the order of 10% of the inducer tip velocity. The LPFTP inducer with flowliner geometry is analyzed to represent the time-periodic nature of the flow field. The computed results show dominant 4N unsteadiness at a fixed location as shown in figure 3(a). Figure 3(b) shows maximum and minimum non-dimensional pressure values recorded from the experimental data. Comparisons between CFD results and hot fire test data also show good correlation in the non-dimensional pressure amplitudes.

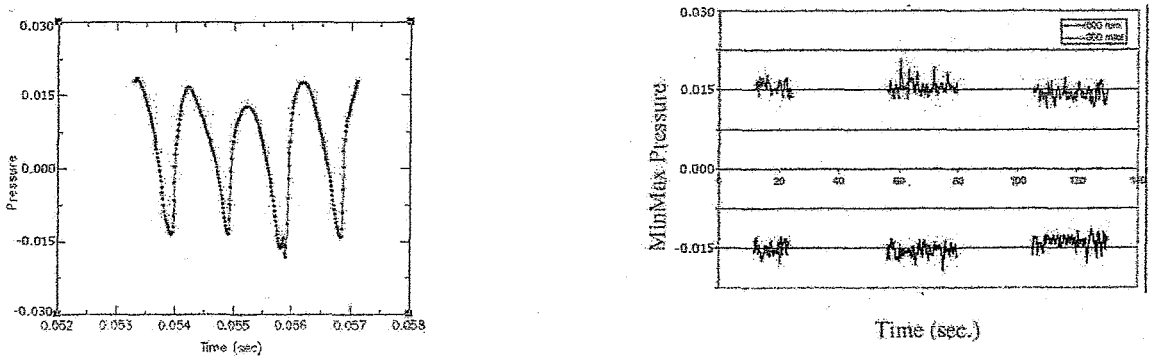

(a) (b)

Figure 3. Time history of non-dimensional pressure during one inducer rotation (model I, 14th inducer rotation), and Min/Max values of non-dimensional pressure in hot fire test.

In the full-length version, further details of the high-fidelity computational procedures will be discussed using the example described above.

References

1. Kiris, C., and Kwak, D., 'Parallel Unsteady Turbopump Simulations for Reusable Launch vehicle,' Frontiers of Computational Fluid Dynamics 2002, Caughey, D.A. and Hafez, M., ed, World Scientific, 2002.
2. Kiris, C., Kwak, D., and Rogers, S., ' Incompressible Navier-Stokes Solvers in Primitive Variables and Their Applications to Steady and Unsteady Flow Simulations,' Numerical Simulations of Incompressible Flows, Hafez, M., ed, World Scientific, 2003.
3. Rogers, S. E., Kwak, D. and Kiris, C., "Numerical Solution of the Incompressible Navier-Stokes Equations for Steady and Time-Dependent Problems," AIAA Journal, Vol. 29, No. 4, pp. 603-610, 1991.

Slides for
A paper to be presented at
The Fourth International Conference on CFD, Ghent Belgium, July 10-14, 2006

"Unsteady Flow Simulation of High Speed Turbopumps"
By Cetin Kiris, Dochan Kwak, William Chan, and Jeff Housman

Export Control Information

All the material in these presentations are in public domain and have been disseminated previously in the following publications and meeting presentations

- Kiris, et. al. Super Computing 2004
- D. Kwak and C. Kiris, "Successes and Challenges of Incompressible Flow Simulation" presented at the 16th AIAA Computational Fluid dynamics Conference, Orlando, FL, June 23-26, 2003
- Super Computing 2004
- Kwak, D., Kiris, C. and Kim, C.S., 'Computational Challenges of Viscous Incompressible Flows,' *Computers & Fluids* **34**, pp283-299, 2005.
- The material in this presentation has been presented to numerous visitors to NAS facility at Ames including the presentation material to Dr. Sato, Director of Earth Simulator, Japan on April 28, 2005

Unsteady Flow Simulation of High Speed Turbopumps

Cetin Kiris, Dochan Kwak, William Chan, and Jeff Housman
NASA Advanced Supercomputing Division (NAS)
NASA Ames Research Center

ICCFD4 Conference, Ghent, Belgium
July 10-14, 2006

OUTLINE

- Liquid Rocket Subsystem Simulation / Background
- Flow Solver / Overset Grid System / Scripting Capability
- High Pressure Fuel Pump Impeller/Diffuser
- Low Pressure Fuel Pump and Flowliners Simulation
  - Performance characterization of the Columbia
- Fuel Feedline System : Test stand / Flight Configuration
- Summary

Liquid Rocket Subsystem Simulation

Goal:

To provide a high-fidelity computational framework for design and analysis of the fuel/oxidizer supply subsystem for liquid rocket propulsion systems.

Objective:

- Decrease design cost
- Improve performance and reliability

  Critical path for:

  -Investigating new designs for future engines.

  -Retrofitting (i.e. determining fuel-line crack issue for Space Shuttle Program)

Modeling and Simulation Challenges:

- Complex geometry: CAD-to-solution scripting capability.
- *Boundary layer transition and separation*
- Transient flow phenomena.
- Multi-phase flow environment
- Tip Vortices
- Parallel, scalable computational procedure.
- Systems analysis capability for trade study in designing components
- Accurate prediction of flow-induced vibration

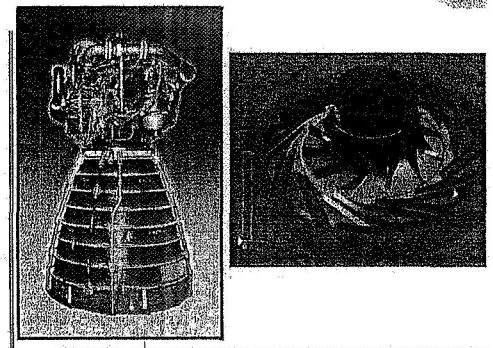

UNSTEADY AND TRANSIENT FLOW IN LIQUID ROCKET ENGINE PUMP

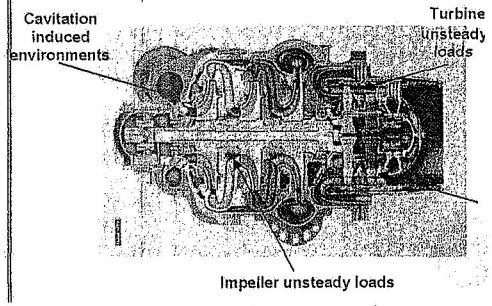

Evolution of Pump Simulation Capability (1983-2006)

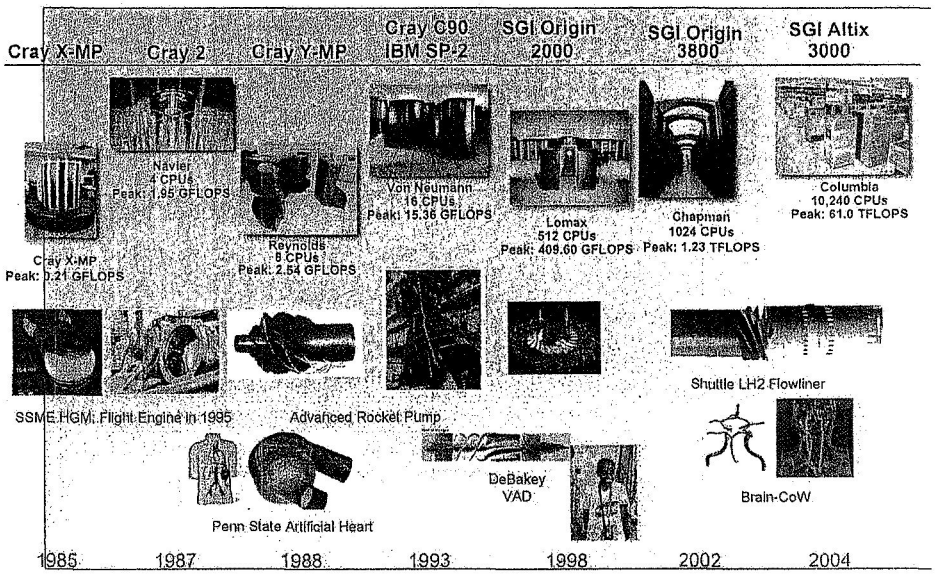

Incompressible Navier-Stokes Solver INS3D

- Finite-difference, structured, overset grid orientation
- Moving grid capability
- Based on method of artificial compressibility
- Both steady-state and time-accurate formulations
- 3rd and 5th-order flux difference splitting for convective terms
- Central differencing for viscous terms
- One- and two-equations turbulence models
- Several linear solvers : GMRES, GS line-relaxation, LU-SGS, GS point-relaxation, ILU(0)..,..

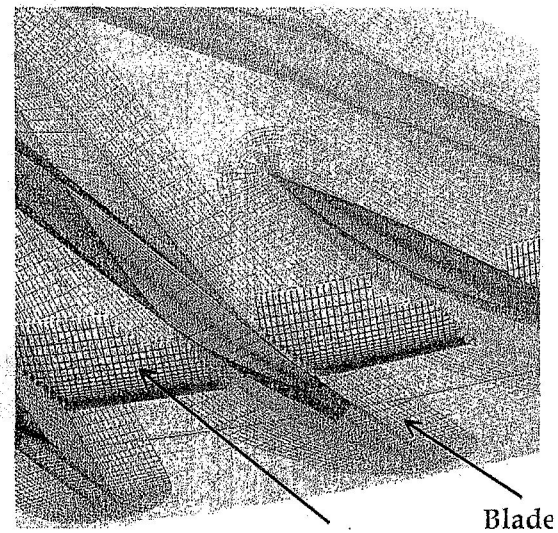

Scripting Capability

SCRIPT DEVELOPMENT FOR TURBOPUMP SIMULATIONS

Motivation

Significant user's effort needed in complex process from geometry to flow solver

Objective

Develop script system to
- generate grids
- create domain connectivity input
- create flow solver input

for different components automatically

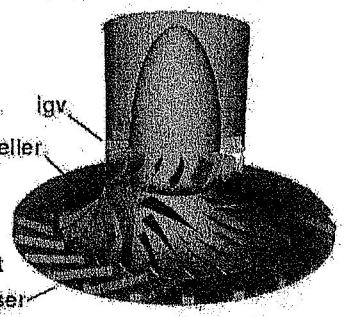

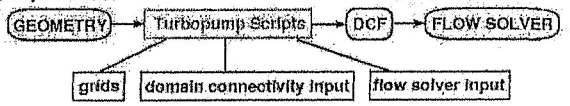

Approach

Develop one script for each component with ring interface between components => easy plug in for different designs and combinations of components

SSME Impeller

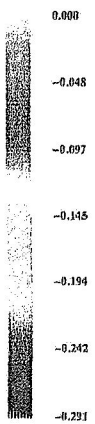

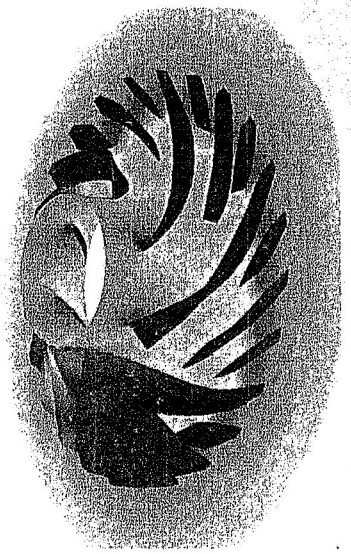

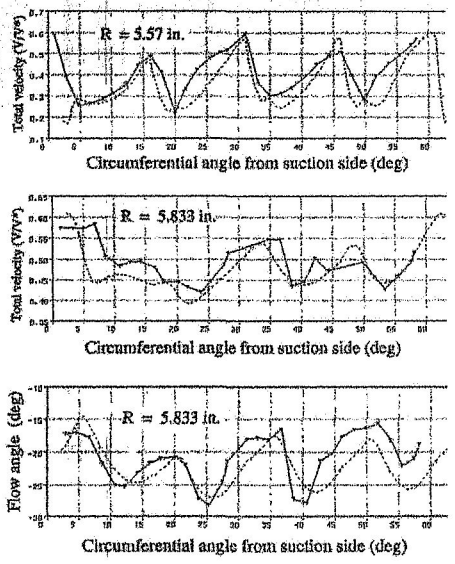

Wide-Range Flow Impeller-Diffuser

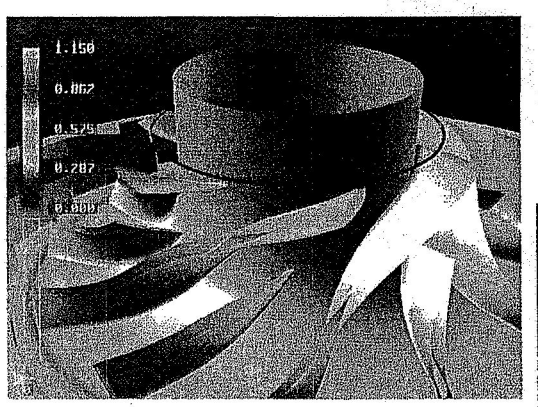

Particle traces are colored by velocity magnitude

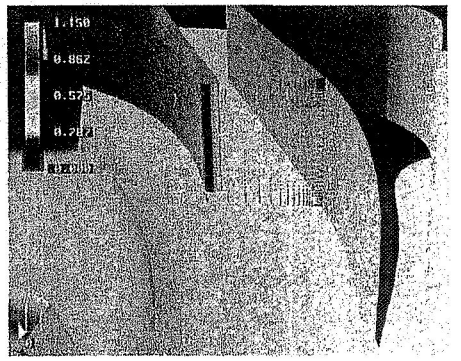

Code INS3D
34.3 Million Grid Points, 114 Zones
One Rotation takes 12 hours on Columbia by using128 CPU's

Flowliner Crack Analysis

-The pressure difference between pressure side and suction side of the inducer blade causes backflow near the tip.

-Extent of backflow varies with inducer design and operating conditions. The backflow also generates pre-swirl in the flow approaching the inducer.

-Investigate the effects of backflow in flowliner models.

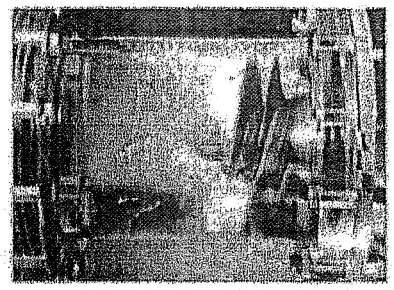

Inducer Experiment:Courtesy MSFC

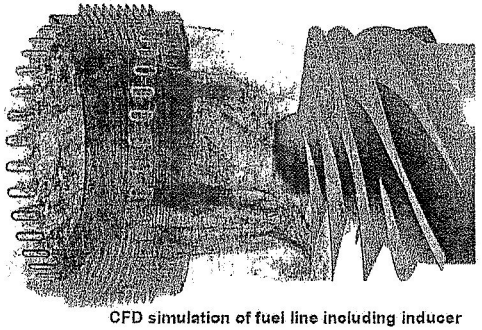

CFD simulation of fuel line including inducer

Flowliner Computational Model

-Flowliner + Straight duct + inducer with 4 long and 4 short blades.
-66 Million Grid points with 264 overlapped zones.

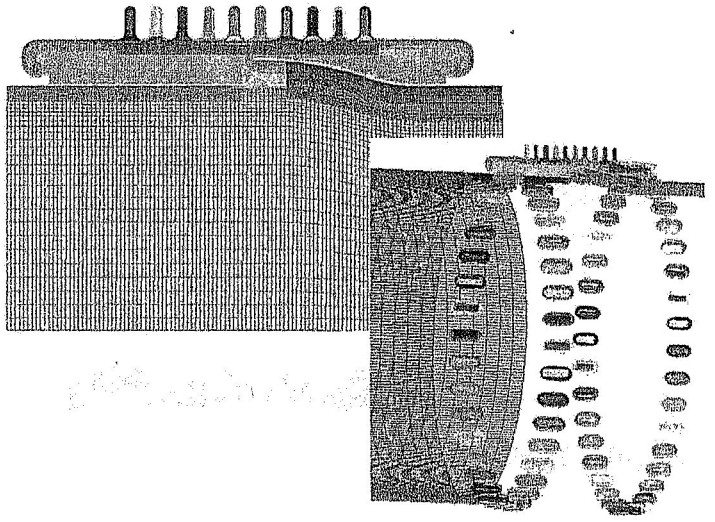

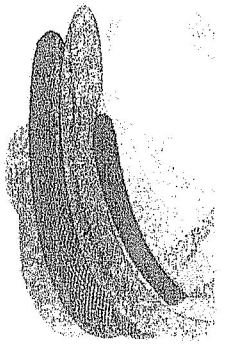

Flowliner CFD Analysis

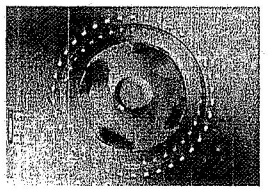

Strong backflow causing high-frequency pressure oscillations

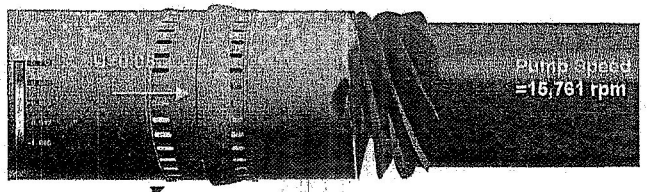

UPSTEREAM LINER

DOWNSTREAM LINER

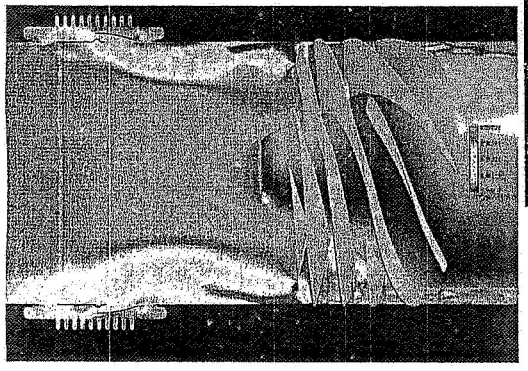

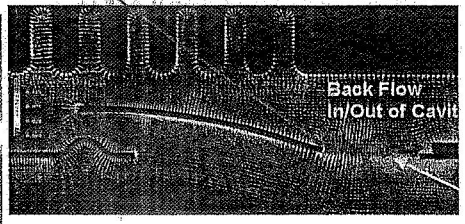

Damaging frequency on flowliner due to LH2 pump back flow has been quantified in developing flight rationale for the flowliner.

Flowliner Computed Results

- Pressure contours at an instantaneous time.

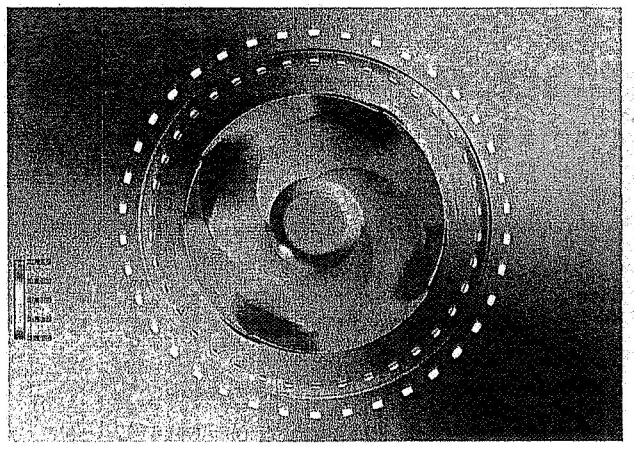

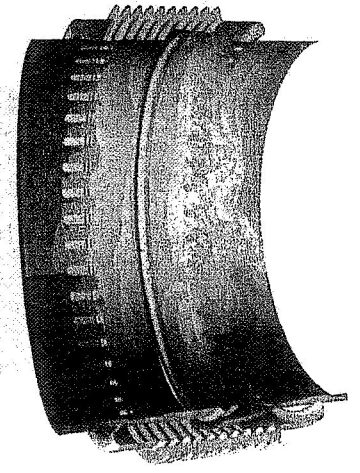

Min/Max Pressure Near Downstream Liner

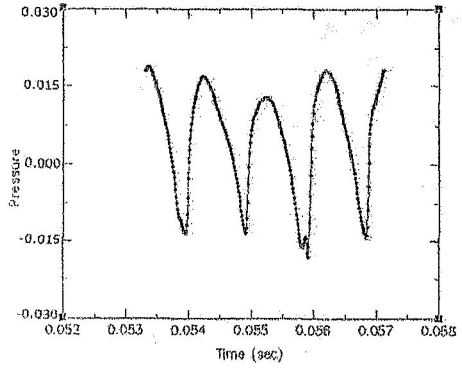

Computation: Pressure During one Rotation

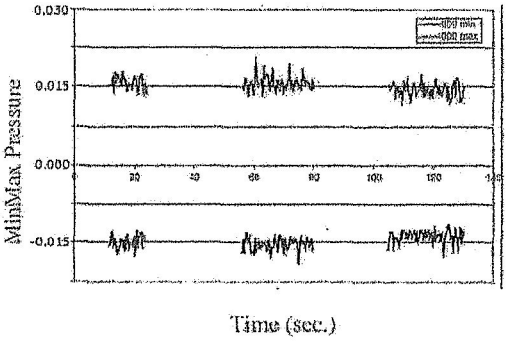

Experiment: Min/Max Pressure

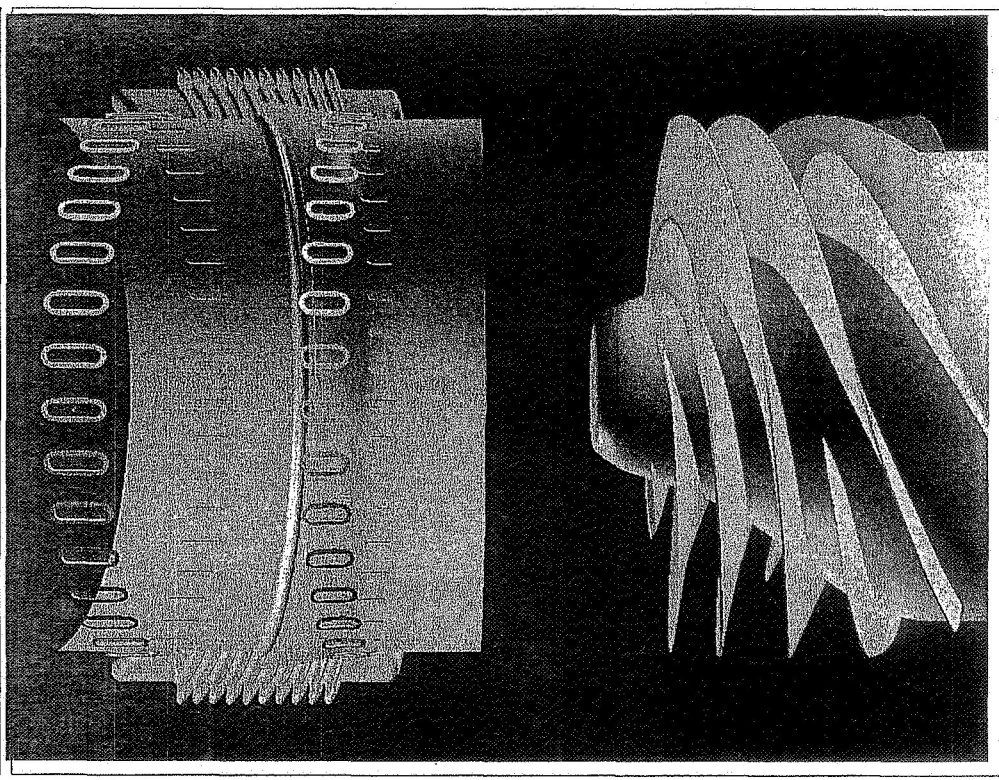

Flowliner Analysis

Particle Traces Colored by Axial Velocity Magnitude

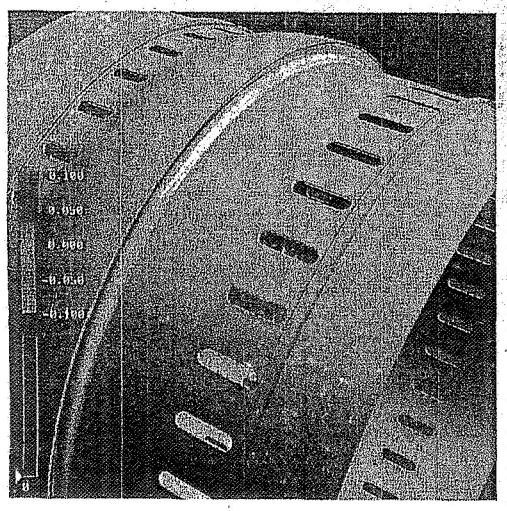

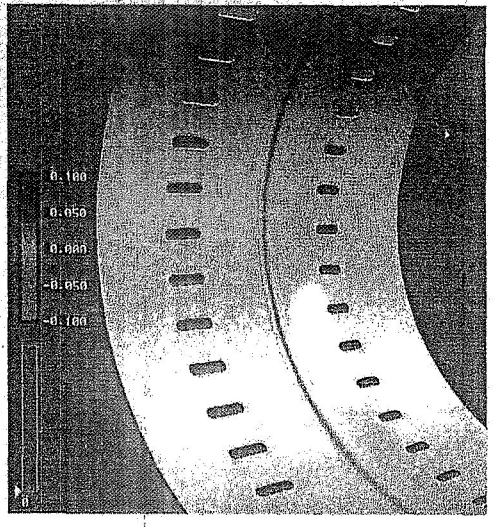

Flowliner Analysis

Particle Traces Colored by Axial Velocity Magnitude

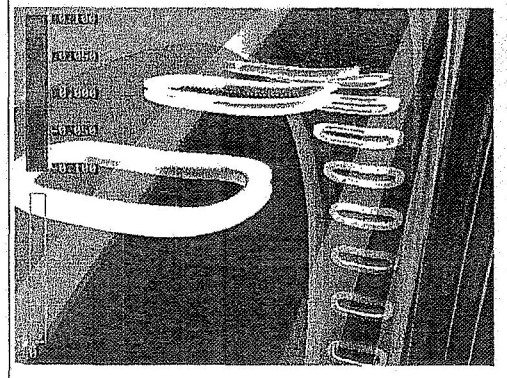

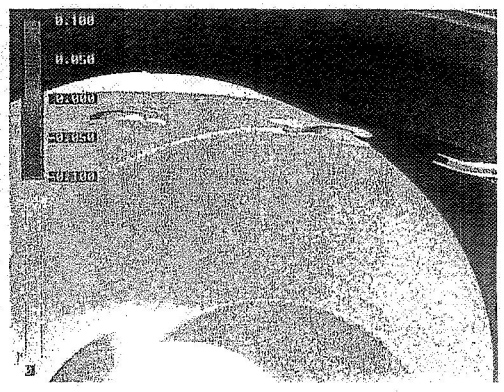

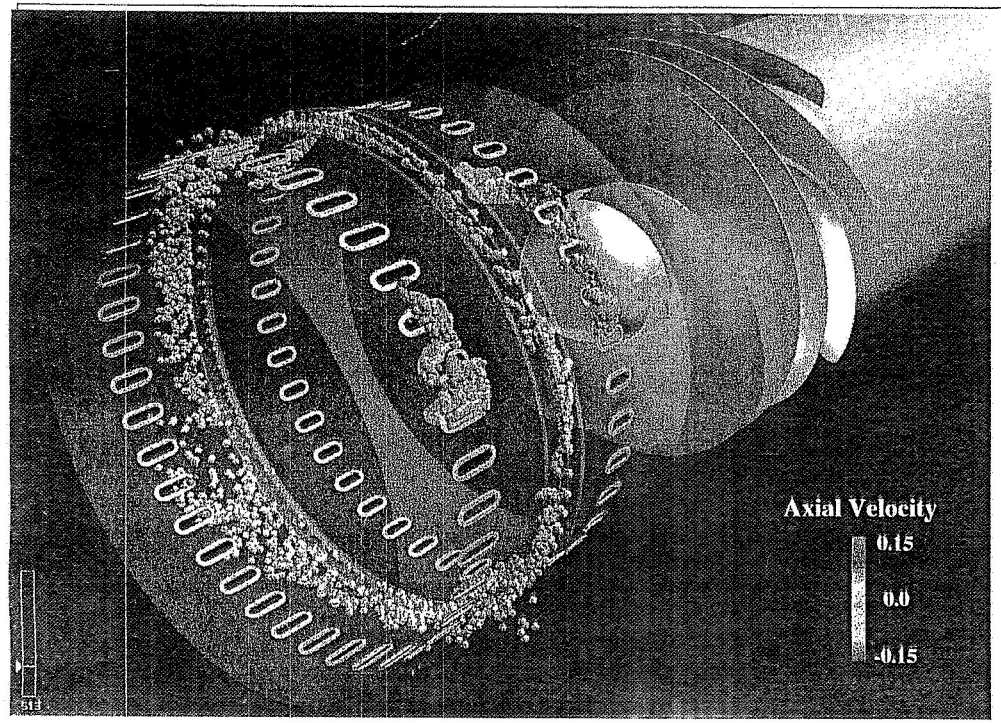

Flowliner Analysis

- Velocity vectors at an instantaneous time.

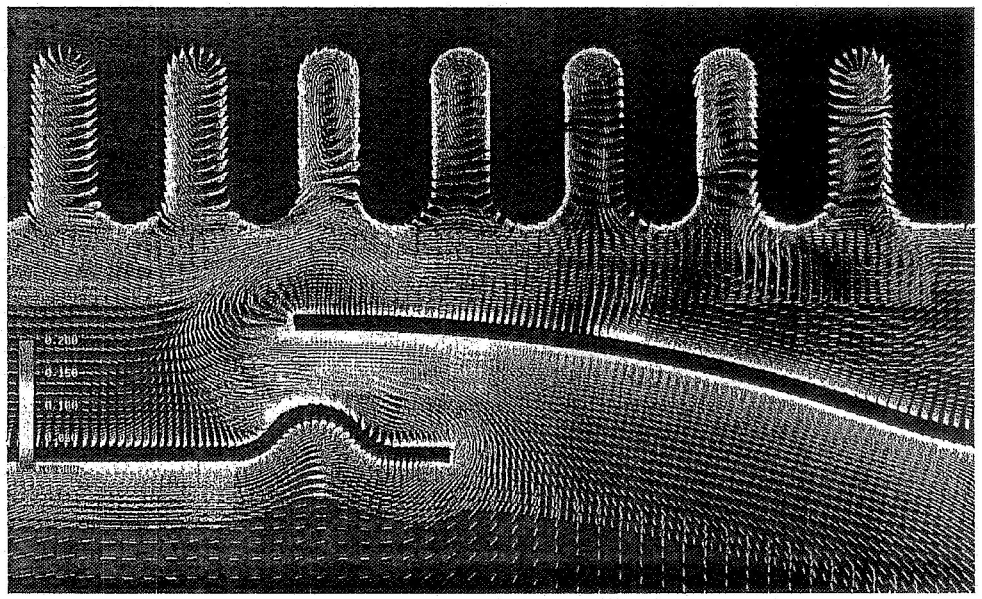

INS3D Parallelization

INS3D-MPI / Open MP

MPI (coarse grain) + OpenMP (fine grain)

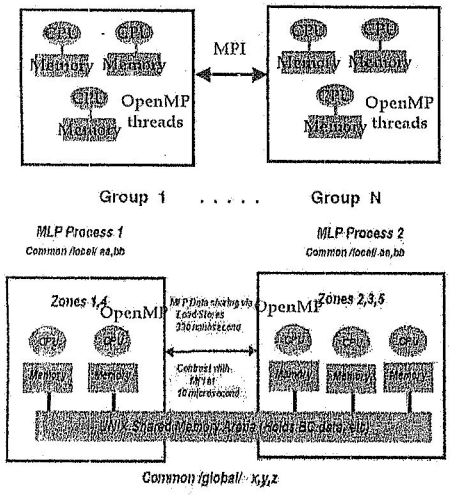

INS3D-MLP

TEST CASE : LPFTP Flowliner
264 zones / 66 million points

INS3D-MPI/OpenMP vs. -MLP/OpenMP

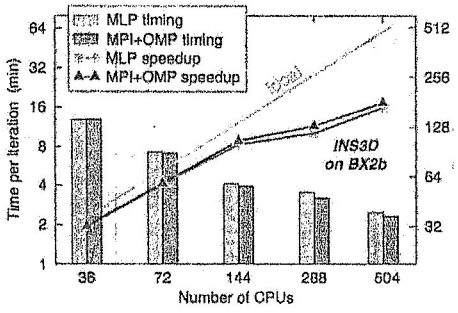

3700 vs BX2: INS3D Performance

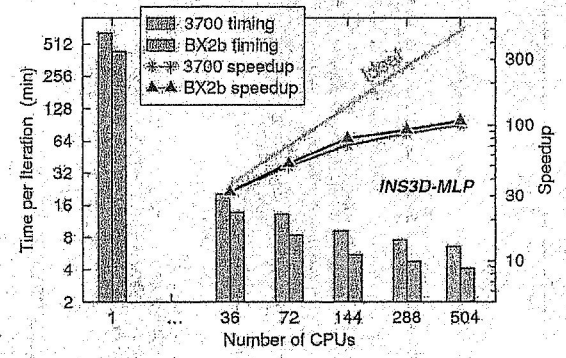

- Except for the first point, number of MLP processes is fixed at 36 and number of OpenMP threads is increased
- On average INS3D runs 50% faster on BX2b than 3700
- Performance scalability of INS3D on BX2b is similar on 3700
- Efficiency beyond 4 OpenMP threads is impacted by remote data access
- Higher performance on BX2b is due to faster clock, larger cache and higher network bandwidth

Multi-Node: INS3D Performance

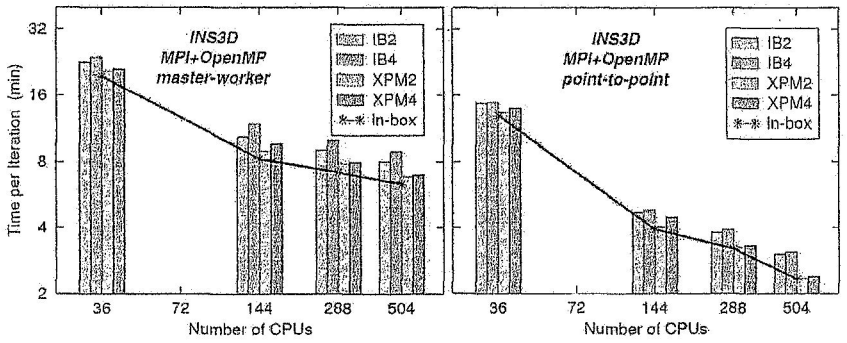

- Execution time via NUMAlink4 generally 15-25% better than InfiniBand
- Total execution time is increased 8-16% from two nodes to four nodes, but is roughly the same from one node to two nodes via NUMAlink4.
- Penalty in communication time increases as number of processors is increased, especially in the master-worker communication approach. The point-to-point communication approach resulted in much better scaling because of better utilization of network bandwidth.

A1 Test Stand

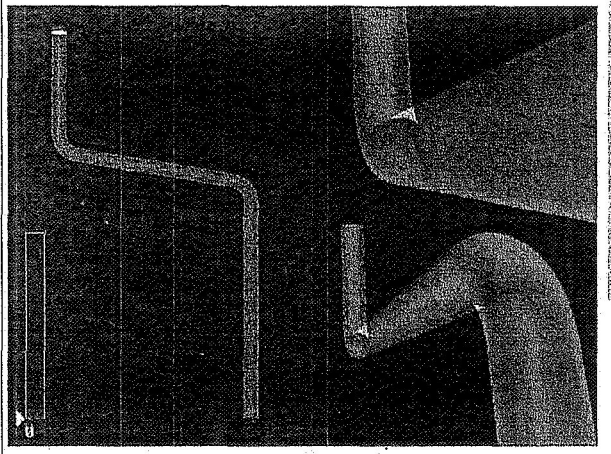

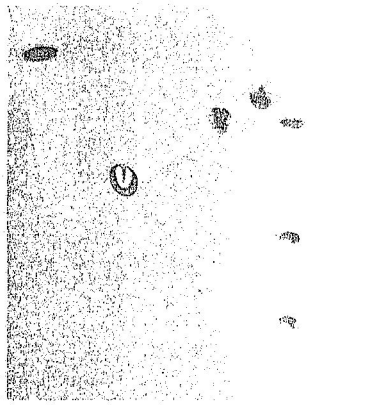

LH_2 Feedline System

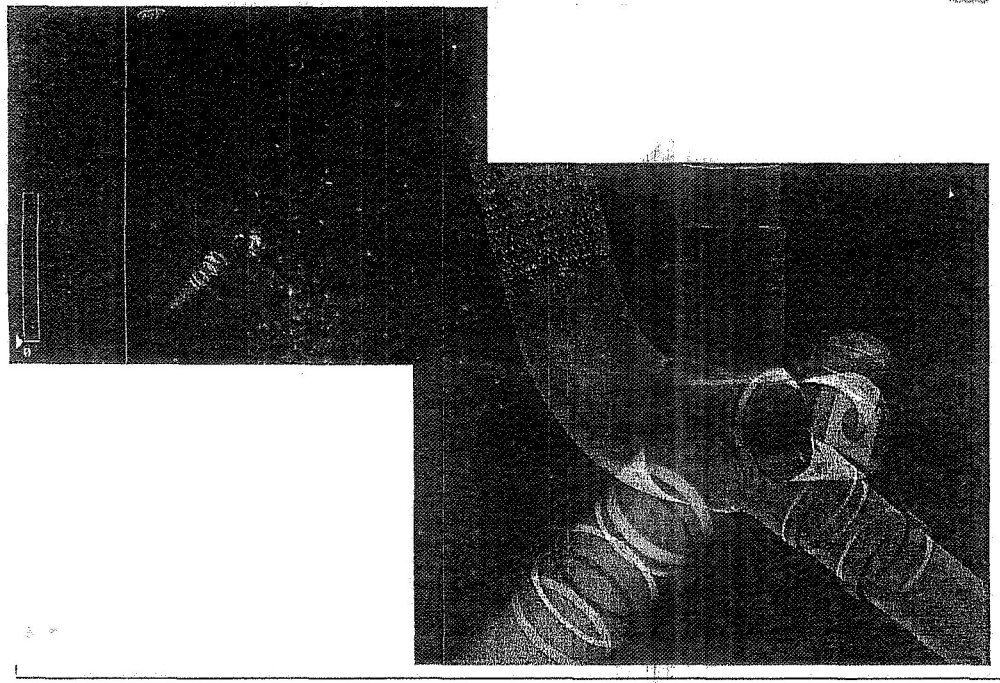

LH_2 Feedline System-Total Velocity

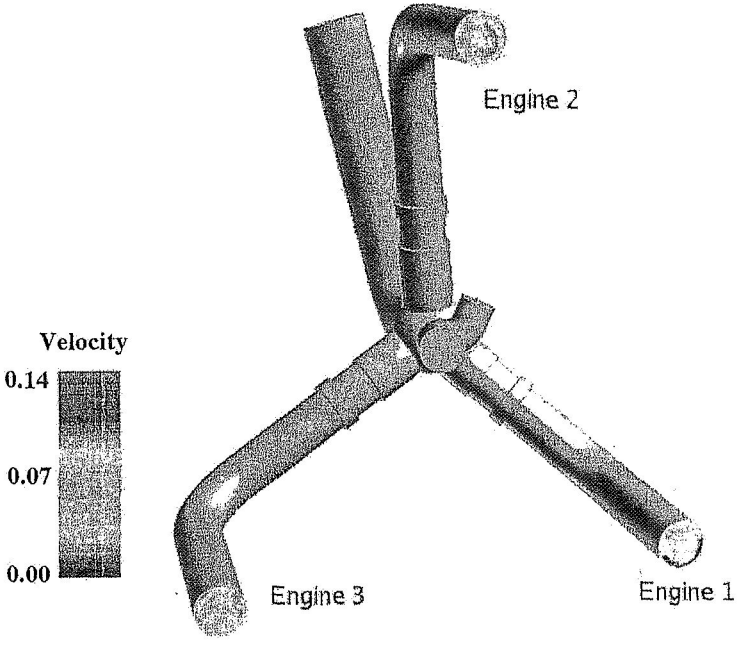

Three-engine Integrated Configuration

- Computational model includes BSTRA joints, detailed flowliner configurations and low pressure fuel pumps for three engines, and the manifold with fuel-line system up to the tank (250+ Million grid points).
- It will quantify variation in incoming flow conditions to the three engines (failure rates for the three engines are not the same).

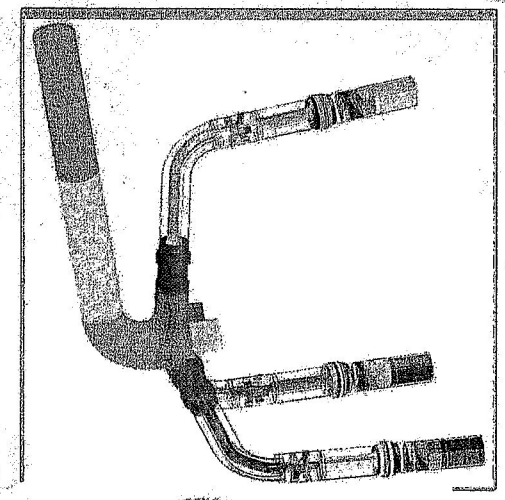

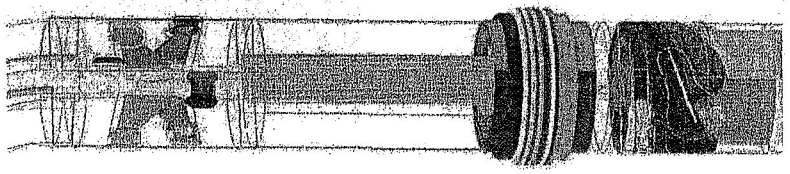

Summary

• High-fidelity turbopump simulations were performed on the Columbia system by using both MLP and MPI/OpenMP hybrid paradigms. Their performances were compared by using single node and multi node calculations.

• The pressure difference between pressure side and suction side of the inducer blade causes backflow near the tip. Extent of backflow interferes with downstream and upstream flowliner.
• The backflow generates pre-swirl in the flow approaching the inducer. Swirl velocity in the cavity is ~10% of inducer tip velocity. The swirl on the duct side of downstream flowliner is stronger than on the duct side of the upstream flowliner.
•Backflow in the duct interacts with the flow in cavity through the flowliner overhang area by creating a strong jet flow (15-20% of tip velocity).

•Incoming flow to the flowliner and LPFTP is more uniform in A1 test stand than in the orbiter manifold.